Symulacja w Badaniach i Rozwoju
Vol. 2, No. 4/2011

Stanisław NOGA
Politechnika Rzeszowska

Roman BOGACZ
Politechnika Krakowska

Free vibration of the Timoshenko beam interacting with the Winkler foundation

1 Introduction

The vibration theory of beams resting on the foundation has great importance in many fields of engineering including the civil and mechanical egineering, and others [1-3]. The majority of previous work in the field present solutions for the free and forced vibration of the Tiomoshenko beam resting on a homogeneous foundation. The beam systems are modeled by simple or complex one – dimensional continuous systems. Fundamental theory of vibration of simple continuous systems is presented in ref. [8]. The problem of free and forced vibration of continuous Timoshenko beams on Winkler–Pasternak foundations is studied in ref. [9]. An interesting investigation related to vibration of a Timoshenko beam resting on a viscoelastic foundation subjected to a distributed moving load is developed in the paper [1]. A similar study devoted to systematization and explanation of some new effects refered to the moving distributed and oscillating load acting on a beam on an elastic foundation are presented in the article [3]. Another paper in the field [2] is devoted to the problem of stability of densley distributed oscillators moving along a Timoshenko beam on an elastic foundation. In the paper [4] the problem of free vibration of a Timoshenko beam partially loaded with distributed mass at an arbitrary position is investigated. Finite element (FE) representation is a useful technique to solve various dynamic problems connected with engineering structures [5]. Among other things the FE technique is utilized in paper [6] to elaborate the solution of the free transverse vibration problem of elastically connected annular double – membrane compound system. This paper describes an investigation of the free vibration of Timoshenko beam resting on an arbitrary variable Winkler foundation. The complete analytical solution of free vibration of this system is described by using the separation of variable method. Then the studies focused on the preparation of the appropriate FE models of the system under consideration are provided. Some results known for the first time are related. This study continues the recent investigations concerning vibration of structures [7].

2 Timoshenko beam on an arbitrary variable elastic foundation

The objective of this study is the formulation of a dynamic model of an uniform Timoshenko beam resting on an elastic foundation. It is assumed that the beam is homogeneous and it has the rectangular cross section. The foundation is composed of two arbitrary variable, massless, elastic regions of the Winkler type (see Fig. 1). The small

vibration with no damping is considered. The equations of motion of the Timoshenko beam interacting with the Winkler foundation can be written in the form [1], [8]:

$$-\frac{\partial}{\partial x}\left(k'A_0G\left(\frac{\partial w_i}{\partial x}-\phi_i\right)\right)+\rho A_0\frac{\partial^2 w_i}{\partial t^2}+k_{fi}w_i=0$$
$$-\frac{\partial}{\partial x}\left(EI\frac{\partial \phi_i}{\partial x}\right)-k'A_0G\left(\frac{\partial w_i}{\partial x}-\phi_i\right)+\rho I\frac{\partial^2 \phi_i}{\partial t^2}=0 \qquad i=1,2 \qquad (1)$$

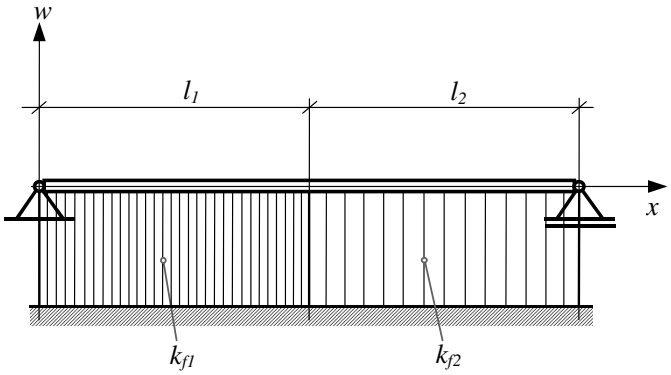

Fig. 1. Physical model of the simple system

where $w_i=w_i(x,t)$ is the transverse beam displacement, $\phi_i=\phi_i(x,t)$ is the rotation of the beam cross section, x, t are the coordinate and the time, k' is the shear correction factor, l_1 and l_2 are the beam dimensions, A_0 is the cross section area, I is the area moment of inertia of the cross section of the beam, ρ is the mass density, k_{fi} is the stiffness modulus of a Winkler elastic foundation, E is the Young's modulus of elasticity and G is the modulus of elasticity in shear (Kirhoff modulus). In these equations i=1 for $0\le x<l_1$ and i=2 for $l_1\le x<l_1+l_2$.

For the simply supported case the corresponding boundary conditions are

$$w_1(0,t)=0,\ EI=\frac{\partial \phi_1(0,t)}{\partial x}=0,\ w_2(l_1+l_2,t)=0,\ EI=\frac{\partial \phi_2(l_1+l_2,t)}{\partial x}=0 \qquad (2a, b)$$

The continuity and equilibrium conditions at $x=l_1$ require

$$w_1(l_1,t)=w_2(l_1,t),\quad \phi_1(l_1,t)=\phi_2(l_1,t) \qquad (3a)$$
$$EI\frac{\partial \phi_1(l_1,t)}{\partial t}=EI\frac{\partial \phi_2(l_1,t)}{\partial t},$$
$$k'A_0G\left(\frac{\partial w_1(l_1,t)}{\partial x}-\phi_1(l_1,t)\right)=k'A_0G\left(\frac{\partial w_2(l_1,t)}{\partial x}-\phi_2(l_1,t)\right) \qquad (3b)$$

The first two relations (3a) are the continuity conditions and the last two (3b) are the equilibrium conditions, respectively.

3 Free vibration analysis

Making use of the classical method of separation of variables, ref. [8], one writes

$$w_i(x,t)=W_i(x)T(t),\quad \phi_i(x,t)=F_i(x)T(t),\quad T(t)=A\cos(\omega t)+B\sin(\omega t),\quad i=1,2 \tag{4a, b, c}$$

where ω is the circular frequency of the system. Introducing solutions (4) into Eq. (1) we obtain the following relations:

$$W_i''(x)+a_iW_i(x)-F_i'(x)=0,\quad F_i''(x)+bW_i'(x)-c\,F_i(x)=0,\quad i=1,2 \tag{5a, b}$$

where

$$a_1=\omega^2\frac{\rho}{k'G}-\frac{k_{f1}}{k'A_0G},\quad a_2=\omega^2\frac{\rho}{k'G}-\frac{k_{f2}}{k'A_0G},\quad b=\frac{k'A_0G}{EI},\quad c=\omega^2\frac{\rho}{E}-\frac{k'A_0G}{EI} \tag{6}$$

and the prime refers to derivative of the function to x. By eliminating the functions $F_i(x)$ (i=1,2) from the equations (5a–b) one can get an equation for transverse displacement $W_1(x)$ and $W_2(x)$ in the form

$$W_1^{(IV)}(x)+(a_1+b+c)W_1''(x)+a_1cW_1(x)=0 \tag{7a}$$

$$W_2^{(IV)}(x)+(a_2+b+c)W_2''(x)+a_2cW_2(x)=0 \tag{7b}$$

After simplification, the boundary conditions in terms $W_i(x)$ become

$$W_1(0)=0,\quad W_1''(0)+aW_1(0)=0,\qquad W_2(l_1+l_2)=0,\quad W_2''(l_1+l_2)+aW_2(l_1+l_2)=0 \tag{8}$$

And likewise the continuity and equilibrium conditions at $x=l_1$ in terms $W_i(x)$ take the form

$$W_1(l_1)=W_2(l_1),\quad W_1'''(l_1)+(a_1+b)W_1'(l_1)=W_2'''(l_1)+(a_2+b)W_2'(l_1) \tag{9a}$$

$$W_1''(l_1)+a_1W_1(l_1)=W_2''(l_1)+a_2W_2(l_1),$$

$$W_1'''(l_1)+(a_1+b+c)W_1'(l_1)=W_2'''(l_1)+(a_2+b+c)W_2'(l_1) \tag{9b}$$

In this study the case where the natural frequencies are below the critical value is analysed. As mentioned earlier the beam is interacting with the Winkler foundation. These assumptions impose the following restrictions on the value of the frequency range

$$\frac{k_{f1}}{\rho A_0}<\omega^2<\frac{k'AG}{\rho I},\qquad \frac{k_{f2}}{\rho A_0}<\omega^2<\frac{k'AG}{\rho I} \tag{10}$$

where $(k'AG)/(\rho I)$ is the critical value of the natural frequencies whereas the values $(k_{f1})/(\rho A_0)$ and $(k_{f2})/(\rho A_0)$ are the lower limits of the frequency. Conditions (10) guarantee the harmonic type of free vibration. General solution for this case can be expressed as

$$W_i(x)=D_{i1}\cos(\lambda_{i1}x)+D_{i2}\sin(\lambda_{i1}x)+D_{i3}\cosh(\lambda_{i2}x)+D_{i4}\sinh(\lambda_{i2}x),\quad i=1,2 \tag{11}$$

where

$$2\lambda_{i1}^2 = \alpha - \beta_i + \sqrt{(\gamma+\beta_i)^2+\eta_i}\,,\quad 2\lambda_{i2}^2 = -\alpha + \beta_i + \sqrt{(\gamma+\beta_i)^2+\eta_i}\,,\quad i=1,2 \tag{12}$$

and

$$\alpha = \omega^2\rho\left(\frac{1}{k'G}+\frac{1}{E}\right),\ \gamma = \omega^2\rho\left(\frac{1}{E}-\frac{1}{k'G}\right),\ \beta_i = \frac{k_{fi}}{k'A_0G},\ \eta_i = \frac{4}{EI}\left(\omega^2\rho A - k_{fi}\right),\quad i=1,2 \tag{13}$$

Substituting equations (11) into equations (9), the following matrix relation is obtained

$$\mathbf{T_1}\begin{bmatrix} D_{11} \\ D_{12} \\ D_{13} \\ D_{14} \end{bmatrix} = \mathbf{T_2}\begin{bmatrix} D_{21} \\ D_{22} \\ D_{23} \\ D_{24} \end{bmatrix} \tag{14}$$

where

$$\mathbf{T_1} = \begin{bmatrix} \cos(\lambda_{11}l_1) & \sin(\lambda_{11}l_1) & \cosh(\lambda_{12}l_1) & \sinh(\lambda_{12}l_1) \\ (\lambda_{11}^3-(a_1+b)\lambda_{11})\sin(\lambda_{11}l_1) & (-\lambda_{11}^3+(a_1+b)\lambda_{11})\cos(\lambda_{11}l_1) & (\lambda_{12}^3+(a_1+b)\lambda_{12})\sinh(\lambda_{12}l_1) & (\lambda_{12}^3+(a_1+b)\lambda_{12})\cosh(\lambda_{12}l_1) \\ (-\lambda_{11}^2+a_1)\cos(\lambda_{11}l_1) & (-\lambda_{11}^2+a_1)\sin(\lambda_{11}l_1) & (\lambda_{12}^2+a_1)\cosh(\lambda_{12}l_1) & (\lambda_{12}^2+a_1)\sinh(\lambda_{12}l_1) \\ (\lambda_{11}^3-(a_1+b+c)\lambda_{11})\sin(\lambda_{11}l_1) & (-\lambda_{11}^3+(a_1+b+c)\lambda_{11})\cos(\lambda_{11}l_1) & (\lambda_{12}^3+(a_1+b+c)\lambda_{12})\sinh(\lambda_{12}l_1) & (\lambda_{12}^3+(a_1+b+c)\lambda_{12})\cosh(\lambda_{12}l_1) \end{bmatrix} \tag{15}$$

,

$$\mathbf{T_2} = \begin{bmatrix} \cos(\lambda_{21}l_1) & \sin(\lambda_{21}l_1) & \cosh(\lambda_{22}l_1) & \sinh(\lambda_{22}l_1) \\ (\lambda_{21}^3-(a_2+b)\lambda_{21})\sin(\lambda_{21}l_1) & (-\lambda_{21}^3+(a_2+b)\lambda_{21})\cos(\lambda_{21}l_1) & (\lambda_{22}^3+(a_2+b)\lambda_{22})\sinh(\lambda_{22}l_1) & (\lambda_{22}^3+(a_2+b)\lambda_{22})\cosh(\lambda_{22}l_1) \\ (-\lambda_{21}^2+a_2)\cos(\lambda_{21}l_1) & (-\lambda_{21}^2+a_2)\sin(\lambda_{21}l_1) & (\lambda_{22}^2+a_2)\cosh(\lambda_{22}l_1) & (\lambda_{22}^2+a_2)\sinh(\lambda_{22}l_1) \\ (\lambda_{21}^3-(a_2+b+c)\lambda_{21})\sin(\lambda_{21}l_1) & (-\lambda_{21}^3+(a_2+b+c)\lambda_{21})\cos(\lambda_{21}l_1) & (\lambda_{22}^3+(a_2+b+c)\lambda_{22})\sinh(\lambda_{22}l_1) & (\lambda_{22}^3+(a_2+b+c)\lambda_{22})\cosh(\lambda_{22}l_1) \end{bmatrix} \tag{16}$$

The boundary conditions yield

$$\mathbf{K_1}\begin{bmatrix} D_{11} \\ D_{12} \\ D_{13} \\ D_{14} \end{bmatrix} + \mathbf{K_2}\begin{bmatrix} D_{21} \\ D_{22} \\ D_{23} \\ D_{24} \end{bmatrix} = 0 \tag{17}$$

where

$$\mathbf{K_1} = \begin{bmatrix} 1 & 0 & 1 & 0 \\ -\lambda_{11}^2 & 0 & \lambda_{12}^2 & 0 \\ 0 & 0 & 0 & 0 \\ 0 & 0 & 0 & 0 \end{bmatrix},$$

$$\mathbf{K_2} = \begin{bmatrix} 0 & 0 & 0 & 0 \\ 0 & 0 & 0 & 0 \\ \cos(\lambda_{21}(l_1+l_2)) & \sin(\lambda_{21}(l_1+l_2)) & \cosh(\lambda_{22}(l_1+l_2)) & \sinh(\lambda_{22}(l_1+l_2)) \\ -\lambda_{21}^2\cos(\lambda_{21}(l_1+l_2)) & -\lambda_{21}^2\sin(\lambda_{21}(l_1+l_2)) & \lambda_{22}^2\cosh(\lambda_{22}(l_1+l_2)) & \lambda_{22}^2\sinh(\lambda_{22}(l_1+l_2)) \end{bmatrix} \tag{18}$$

By using relation (14), the vector of the constants $[D_{11}\ D_{12}\ D_{13}\ D_{14}]^T$ can be eliminated to give

$$\left(\mathbf{K}_1\mathbf{T}_1^{-1}\mathbf{T}_2+\mathbf{K}_2\right)\begin{bmatrix}D_{21}\\D_{22}\\D_{23}\\D_{24}\end{bmatrix}=0 \tag{19}$$

Determinant equation in the natural frequencies is obtained from the condition of nontrivial solution. It yields the secular determinant

$$\left|\mathbf{K}_1\mathbf{T}_1^{-1}\mathbf{T}_2+\mathbf{K}_2\right|=0 \tag{20}$$

where the roots of the determinantal equation (20) $\omega=\omega_n$ (n=1,2,3,…) are the exact natural frequencies. The corresponding eigenvectors of equation (19) together with equation (14) determine the eigenfunctions in the form of equations (11). The eigenfunctions give the mode shapes of the simply supported beam on the Winkler foundation.

4 The finite element representations of the system

In this section the finite element (FE) models are formulated to discretize the continuous model determined by the equations (1). The equations of motion are first transformed into a set of independent or decoupled differential equations cast in modal generalized coordinates through the use of the mode shapes of the structure. The response of the system is then obtained by superimposing the solutions of the decoupled modal equations [5]. To find the eigenpairs (eigenvalue, eigenvector) referred to the natural frequencies and corresponding mode shapes of the system, the block Lanczos method is employed [5]. In this work the analytical solution is regarded as exact, compared to the FE models, which are treated as an approximation of the accurate system.

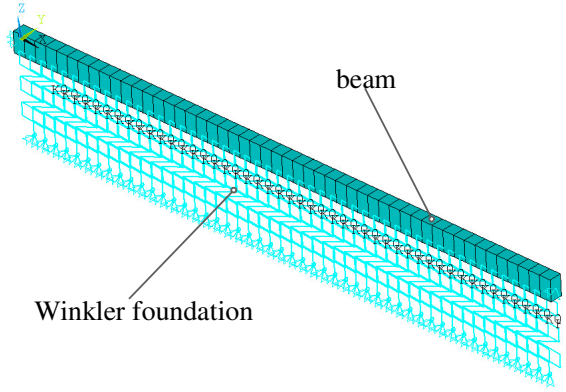

Fig. 2. The first finite element model of the system

The first FE model consists of the simply supported beam divided into 400 finite elements. The two node beam element (beam44) with six degrees of freedom in each node and with the element shear deformation option is used to realize the beam. The Winkler foundation is modeled by a finite number of parallel massless springs. The stiffness modulus k_{Si} of each spring can be receive from the relation [6] and [7].

$$k_{Si} = \left(k_{fi} L_i\right)/b_i, \quad i = 1,2 \tag{21}$$

where L_i is the dimension of the i_{th} foundation part and b_i is the number of the springs modeled that segment of foundation. The spring – damper (combin14) element defined by two nodes is used to realize the Winkler foundation. The element damping capability are neglected. Each i_{th} part of the foundation consists of 200 combin elements. The prepared model is shown in Fig. 2.

In the second FE model case the beam is modeled as the solid body with taking into account the structural geometry of the beam. The eight node hexahedron (solid185) element with three degrees of freedoom in each node is used to realize the beam. The Winkler layer is modeled as for the first FE model. The prepared model consists of 3000 solid elements, and 156 combin elements, respectively.

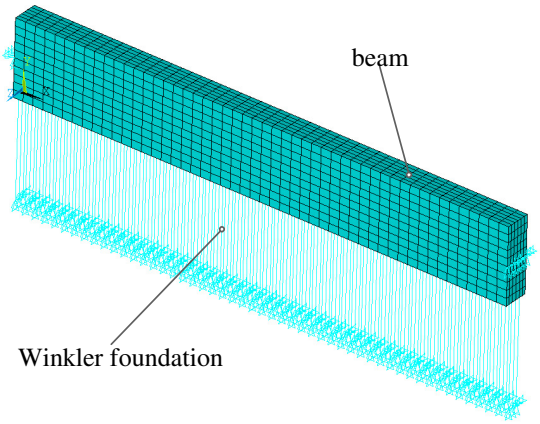

Fig. 3. The second finite element model of the system

The third FE model of the system under study is the same as the first, but the element type modeled the beam is different. In this case the solid body is modeled by the solid45 element (eight node hexahedron with three degrees of freedom in each node).

The difference between the accurate and the FE models is defined by

$$\varepsilon_n = \left(\omega_n^f - \omega_n^c\right)/\omega_n^c \cdot 100\,\% \tag{22}$$

where ω_n^f and ω_n^c are the natural frequencies of the FE and exact models, respectively. Relation (22) is the so–called frequency error [5], [6].

5 Numerical analysis

Numerical solutions for free vibration analysis of the Timoshenko beam resting on Winkler foundation models suggested earlier, are calculated. In the present study, the needed calculations are executed for the exampled beam parameters presented in the reference [8]. For each approach, only the first eight natural frequencies and mode shapes are discussed and compared for these models. The special case where the Winkler foundation modulus of the second foundation region is equal zero, i.e. k_{f2}=0 is

analyzed. The next assumption is that the dimensions of each foundation regions are the same, i.e. $l_1=l_2=l$. Furthermore to compare the achieved results with the ref. [8], in the first instance for each case, the computation for the simply supported beam without the foundation (i.e. $k_{f1}=0$) are executed. Due to space limitation only the most interesting mode shapes of vibration are presented in the Appendix. Parameters characterizing the system used in the calculations are demonstrated in Table 1. In Table 1, d and s are, respectively, the deep and wide of the beam; ν is the Poisson ratio.

Table 1. Parameters characterizing the system under consideration

d [m]	s [m]	I [m^4]	A_0 [m^2]	E [Pa]	ν	k'	ρ [N/m^3]	l [m]
0.15	0.05	$1.4\cdot10^{-5}$	$7.5\cdot10^{-3}$	$2.07\cdot10^{11}$	0.305	5/6	$7.65\cdot10^{4}$	0.5

For the continuous model the natural frequencies are determined from numerical solution of the equation (20). The results of the calculation of the natural frequencies are displayed in Table 2. Worth pointing out is the fact that results presented in the first row of the Table 2 have excellent agreement with the ref. [8]. In the third row of this table there is the limiting value of the Winkler foundation modulus k_{f1} for which the condition (10) is still satisfied, i.e. harmonic type of free vibration can be executed for this case. This value is selected experimentally by numerical simulation. For the higher value of the k_{f1} it is impossible to determine the first natural frequency of the system under study by using equation (20) (see last row of the Table 2).

Table 2. Natural frequencies of the studied system ω_n [Hz] (analytical solution)

n / k_{f1} [N/m^2]	1	2	3	4	5	6	7	8
0	107.88	393.65	787.51	1237.64	1715.17	2205.26	2700.33	3196.51
$6\cdot10^6$	108.49	393.81	787.59	1237.69	1715.22	2205.29	2700.34	3196.54
$4.93\cdot10^8$	147.58	407.21	793.89	1241.67	1718.07	2207.52	2702.17	3198.08
$6\cdot10^9$	-	576.29	862.13	1288.14	1749.90	2232.97	2722.70	3215.77

The natural frequencies and the frequency errors obtained by using the first FE model of the system under investigation are presented in Tables 3 – 4, respectively. For each value of the stiffness modulus k_{f1}, the best compatibility with analytical solution is obtained for the first natural frequency. The frequency error grows in parallel with increase the number of the natural frequencies.

Table 3. Natural frequencies of the system under study ω_n [Hz] (the first FE model)

n / k_{f1} [N/m^2]	1	2	3	4	5	6	7	8
0	108.77	404.31	825.43	1321.1	1859.4	2421.9	2998.1	3582.0
$6\cdot10^6$	109.37	404.47	825.51	1321.1	1859.4	2421.9	2998.2	3582.0
$4.93\cdot10^8$	148.50	417.43	831.46	1324.8	1861.9	2423.8	2999.7	3583.3
$6\cdot10^9$	287.97	582.49	896.33	1366.9	1890.4	2445.8	3017.3	3598.2

Table 4. Frequency error ε_n [%] (the first FE model)

n / k_{f1} [N/m^2]	1	2	3	4	5	6	7	8
0	0.825	2.708	4.815	6.744	8.409	9.824	11.027	12.059

$6 \cdot 10^6$	0.811	2.707	4.815	6.739	8.406	9.822	11.031	12.565
$4.93 \cdot 10^8$	0.623	2.509	4.732	6.695	8.372	9.797	11.011	12.045
$6 \cdot 10^9$	-	1.076	3.967	6.114	8.029	9.531	10.82	11.892

Tables 5 – 6 show the results obtained for the second FE model case. In this instance the achieved results are better as in the first FE model case. It is especially referred to the first seven natural frequencies.

Table 5. Natural frequencies of the system under study ω_n [Hz] (the second FE model)

n k_{fl} [N/m^2]	1	2	3	4	5	6	7	8
0	107.70	389.65	771.67	1198.5	1636.5	2062.2	2457.7	2808.9
$6 \cdot 10^6$	108.30	389.80	771.74	1198.6	1636.5	2062.3	2457.8	2808.9
$4.93 \cdot 10^8$	147.17	402.39	777.85	1202.4	1639.4	2064.5	2459.7	2810.4
$6 \cdot 10^9$	284.05	558.81	841.70	1244.5	1670.1	2089.2	2480.5	2826.0

Table 6. Frequency error ε_n [%] (the second FE model)

n k_{fl} [N/m^2]	1	2	3	4	5	6	7	8
0	-0.167	-1.016	-2.011	-3.162	-4.587	-6.487	-8.985	-12.126
$6 \cdot 10^6$	-0.175	-1.018	-2.012	-3.158	-4.590	-6.484	-8.982	-12.127
$4.93 \cdot 10^8$	-0.278	-1.184	-2.020	-3.163	-4.579	-6.479	-8.973	-12.122
$6 \cdot 10^9$	-	-3.033	-2.370	-3.388	-4.560	-6.439	-8.896	-12.121

Results presented in Tables 7 – 8 are achieved by using the third FE model case. A bit worse compatibility with the exact model compared with the second FE model case only for the first natural frequency of vibration is observed. And these results are more satisfied as in first FE model instance.

Table 7. Natural frequencies of the system under study ω_n [Hz] (the third FE model)

n k_{fl} [N/m^2]	1	2	3	4	5	6	7	8
0	107.56	389.71	773.20	1203.5	1647.5	2082.2	2486.8	2838.3
$6 \cdot 10^6$	108.15	389.86	773.28	1203.6	1647.6	2082.2	2486.8	2838.3
$4.93 \cdot 10^8$	147.06	402.44	779.37	1207.3	1650.4	2084.4	2488.7	2839.8
$6 \cdot 10^9$	283.99	558.82	843.00	1249.1	1680.7	2108.7	2509.3	2855.3

Table 8. Frequency error ε_n [%] (the third FE model)

n k_{fl} [N/m^2]	1	2	3	4	5	6	7	8
0	-0.297	-1.001	-1.817	-2.758	-3.945	-5.580	-7.908	-11.206
$6 \cdot 10^6$	-0.313	-1.003	-1.817	-2.754	-3.942	-5.582	-7.908	-11.207
$4.93 \cdot 10^8$	-0.352	-1.171	-1.829	-2.768	-3.939	-5.577	-7.900	-11.203
$6 \cdot 10^9$	-	-3.031	-2.219	-3.031	-3.955	-5.565	-7.838	-11.209

For each FE model cases the largest difference between the analytical results and FE solutions can be noticable for the frequency ω_8. Moreover, for each FE model cases, apart from the value of the Winkler foundation modulus, the frequency error grows in parallel

with increase the number of the natural frequencies. For the values of Winkler foundation modulus k_{f1} which are higher than the limiting value (third row of the Table 2), the first natural frequency can be found only by using FE computations. But taking into account the deformation of the mode shape related to such natural frequency (see Fig. 4b and Fig. 6b), it can be visible that it is not harmonic type of free vibration. Presented results show that if the system is approximated by the beam FE model, the natural frequencies approach the exact values from above, and by one of the solid FE model, the natural frequencies approach the exact values from below. It seems that the solid FE model (specially the third FE model) would be better to simulate the system under study.

6 Free vibration analysis of a system modeling railway rail segment

Presented consideration are used to analyse the vibration of the rail – sleeper system. Because produced sleepers are not satisfactory, the presented approach will be helpful to design and manufacture a better rail–sleeper system. An assumed model of the rail–sleeper system is presented in Fig. 4. In this model the collaboration region of the rail and the sleeper is modeled by a massless, linear, elastic foundation of a Winkler type, where k_f and l_p are, the stiffness modulus, and the dimension of the foundation, respectively. The length l_0 is the distance between the sleepers. The influence of the remainder parts of the rails and sleepers on the analyzed system is modelled by spiral springs of stiffness k_R.

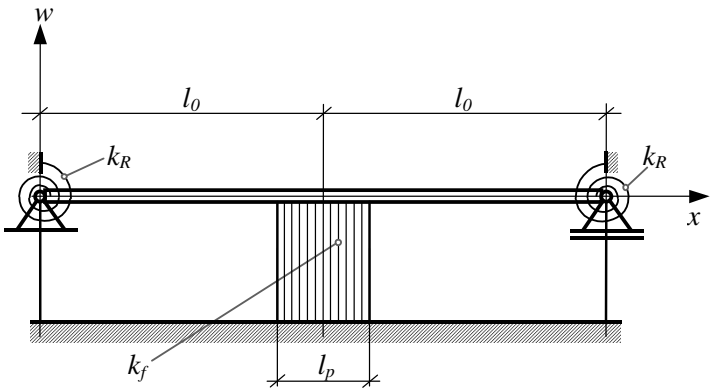

Fig. 4. Physical model of the system

In this section the preliminary studies focused on the free vibration problem of the system under consideration by using the finite element method are presented. For the investigation, the railway rail model UIC 60 E1 which is usually used in track line is assumed. Two FE models of the railway rail are prepared. In both elaborated FE models a complex geometrical shape of the rail are taken into consideration. According to earlier experiences in both cases the rail is modelled by using the solid element (*solid45*). Like in previous case the Winkler foundation is modelled by a finite number of parallel massless springs and it is realized by using spring damper element (*combin14*). Based on the ref. [3] it is assumed that the value of the sleeper – rail system stiffness modulus is equal to $k_p=3\cdot10^7[N/m]$. The stiffness modulus of the Winkler foundation springs is obtained from the relation:

$$k_{p0} = k_p / b_0 \tag{23}$$

where b_0 is number of the springs of the modelled Winkler foundation segment. The spiral springs are modelled by massless rail segments length l_0 and with the proper value of Young's modulus E, and Poisson ratio ν. The elastic connection each spiral spring rail segment with the ground is included (see Fig. 4). Like in previous case the stiffness modulus of the elastic connection of the rail segment is achieved from equation (23).

The first FE model is elaborated for the case where $l_p=(1/8)l_0$. It includes 31200 solid elements (*solid45*) and 198 combin elements (*combin14*), respectively.

The second FE model is prepared for the case where width of the sleeper is equal to $l_p=(1/4)l_0$. The model consists of 31200 solid elements (*solid45*) and 342 combin elements (*combin14*).

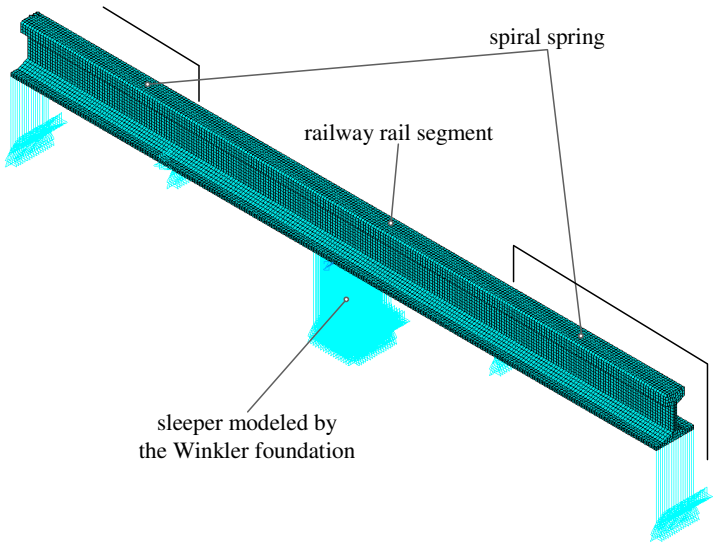

Fig. 5. Finite element model of the system

Table 9 presents the parameters characterizing the railway rail segment under investigation.

Table 9. Parameters characterizing the railway rail segment under consideration

E [Pa]	ν	ρ [kg/m^3]	l_0 [m]
$2.06 \cdot 10^{11}$	0.3	$7.85 \cdot 10^4$	0.65

For each case presented here, only the first three natural frequencies and corresponding mode shapes are discussed. Table 10 shows the results related to the first FE model of the studied system.

Table 10. Natural frequencies of the system under consideration ω_n (the first FE model, $l_p=(1/8)l_0$)

n	1	2	3
ω_n [Hz]	348.76	979.93	1632.4

The natural frequencies presented in Table 11 are referred to the second FE model of the system under consideration.

Table 11. Natural frequencies of the system under consideration ω_n (the second FE model, $l_p=(1/4)l_0$)

n	1	2	3
ω_n [Hz]	348.63	980.24	1632.0

From the analysis of the received results the negligible difference between the natural frequencies from the first FE model and natural frequencies from the second FE model are noticeable. Due to significant shape similarity between the corresponding forms of the FE models, only the mode shapes achieved form the first FE model are presented in the Appendix (Figs. 10 – 12).

Then the numerical calculations are executed for the case where in both elaborated FE models the rail segments modelled the spiral springs include the mass. The remainder components of the FE models are the same as for the previous discussed FE models. Like in previous case, based on the prepared FE models the first three natural frequencies and mode shapes are discussed. In Table 12 the results of calculation referred to the first FE model (with taking into account the mass of the rail segments modelled the spiral springs) are presented.

Table 12. Natural frequencies of the studied system ω_n [Hz] (the first FE model)

n	1	2	3
ω_n [Hz]	253.87	329.56	471.89

Table 13 shows the results related to the second FE model of the system under study.

Table 13. Natural frequencies of the studied system ω_n [Hz] (the second FE model)

n	1	2	3
ω_n [Hz]	253.82	329.57	471.79

In the first FE model case the value of the natural frequencies are almost the same as in the second FE model case. Moreover the substantial shape similarity between the corresponding forms of the FE models are observed. The mode shapes of vibration corresponding to the presented pairs of the natural frequencies obtained from the second FE model are shown in the Appendix (Figs. 13 – 15).

Taking into account presented results of computation corresponding to the system under study, substantial difference between the FE models with the mass rail segments modelled the spiral springs solutions and FE models with massless rail segments modelled the spiral springs results are noticed. For each FE model with massless rail segments related to the spiral springs cases the values of the following natural frequencies are considerably higher compared to each FE model with mass rail segments cases. Moreover the substantial shape differences between the corresponding forms of the FE models are observed (see Figs. 10 – 15). At this stage of search it is not possible to state whether for both analyzed cases there are harmonic type of free

vibration. The future research concerning the elaborating the exact solution of free vibration of the railway rail segment with spiral springs is needed.

7 Conclusions

This paper deals with the free transverse vibration of a simply supported Timoshenko beam attached to arbitrary variable elastic foundation of the Winkler type. The exact solution of the free vibration of the system under study is found by using the separation of variables method. Numerical computations are executed for the special case where the Winkler founation modulus for one of the foundation regions is equal to zero. Then the analytical solution of the system under study is treated as exact, compared to the FE models, which are treated as an approximation of the accurate system. Three FE models of the complex system are investigated. The principal profit of using the FE models is the knowledge related to the value of the anharmonic type natural frequency, which can not be determine
d by using the classical Timoshenko beam theory. At this stage of research it seems that the third FE model would be better to simulate the analyzed Timoshenko beam attached to Winkler foundation. To achieve better consistency between the FE models and the exact solution, further research is needed.

References

1. R. Bogacz, On dynamics and stability of continuous systems subjected to a distributed moving load, *Ingenieur – Archiv* 53 (1983) 243–255.
2. R. Bogacz, S. Nowakowski, K. Popp, On the stability of a Timoshenko beam on an elastic foundation under a moving spring – mass system, *Acta Mechanica* 61 (1986) 117–127.
3. R. Bogacz, W. Czyczuła, Response of beam on visco – elastic foundation to moving distributed load, *Journal of Theoretical and Applied Mechanics* 46 (2008) 763–775.
4. K. T. Chan, X. Q. Wang, Free vibration of a Timoshenko beam partially loaded with distributed mass, *Journal of Sound and Vibration* 206 (1997) 353–369.
5. C. de Silva, *Vibration and Shock Handbook*, Taylor & Francis, Boca Raton, 2005.
6. S. Noga, Free transverse vibration analysis of an elastically connected annular and circular double – membrane compound system, *Journal of Sound and Vibration* 329 (2010) 1507–1522.
7. S. Noga, Free vibrations of an annular membrane attached to Winkler foundation, *Vibrations in Physical Systems*, vol. XXIV (2010) 295–300.
8. S. S. Rao, *Vibration of Continuous Systems*, Wiley, Hoboken, 2007.
9. T. Wang, L. Gagnon, Vibrations of continuous Timoshenko beams on Winkler – Pasternak foundations, *Journal of Sound and Vibration* 59 (1978) 211–220.

Appendix

Graphical visualization of some mode shapes of the systems under study.

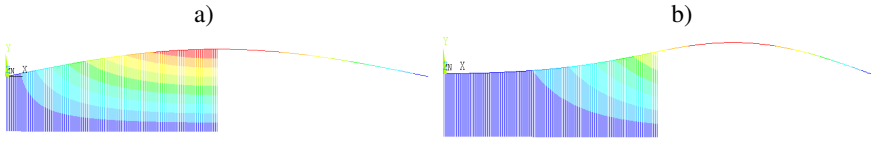

Fig. 6. The mode shapes corresponding to frequency ω_1 (the first FE model); (a) harmonic type of vibration, (b) anharmonic type of vibration

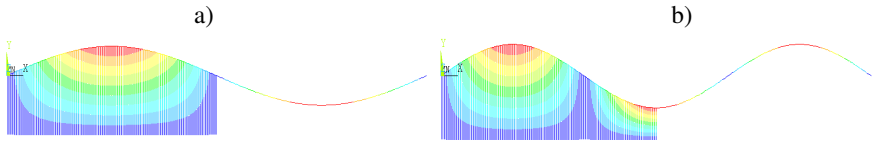

Fig. 7. The mode shapes corresponding to frequencies: (a) ω_2 and (b) ω_3 (the first FE model)

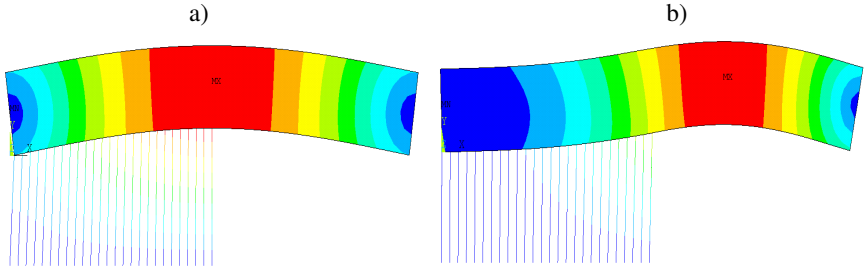

Fig. 8. The mode shapes corresponding to frequency ω_1 (the solid FE model); (a) harmonic type of vibration, (b) anharmonic type of vibration

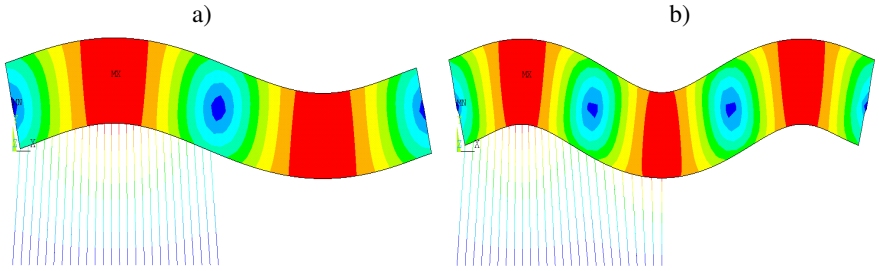

Fig. 9. The mode shapes corresponding to frequencies: (a) ω_2 and (b) ω_3 (the solid FE model)

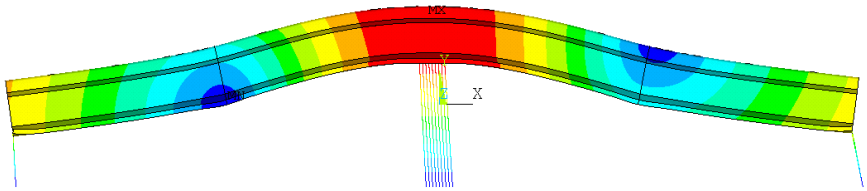

Fig. 10. The mode shapes corresponding to frequency ω_1 (the first FE model of the railway rail, $l_p=(1/8)l_0$)

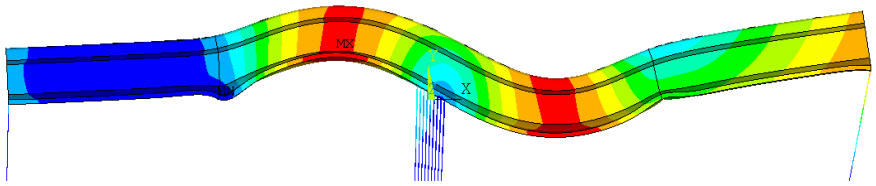

Fig. 11. The mode shapes corresponding to frequency ω_2 (the first FE model of the railway rail, $l_p=(1/8)l_0$)

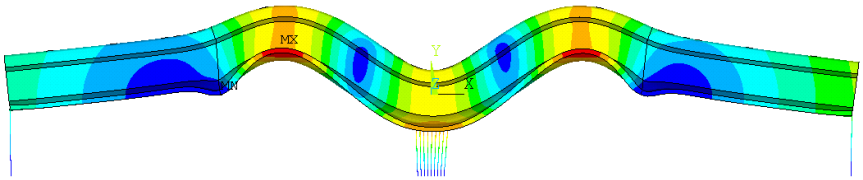

Fig. 12. The mode shapes corresponding to frequency ω_3 (the first FE model of the railway rail, $l_p=(1/8)l_0$)

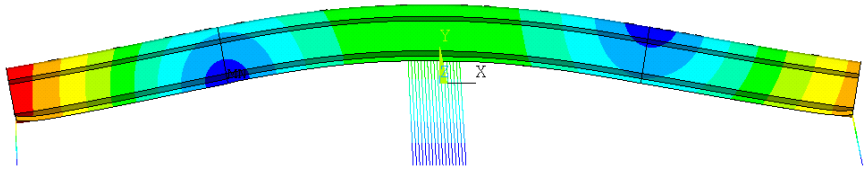

Fig. 13. The mode shapes corresponding to frequency ω_1 (the second FE model of the railway rail, $l_p=(1/4)l_0$)

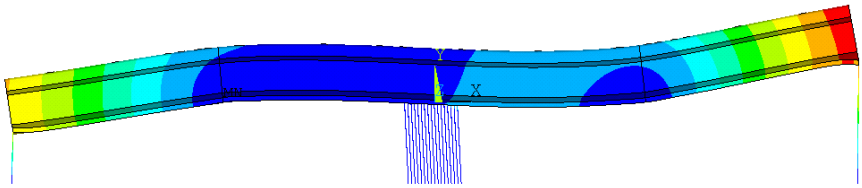

Fig. 14. The mode shapes corresponding to frequency ω_2 (the second FE model of the railway rail, $l_p=(1/4)l_0$)

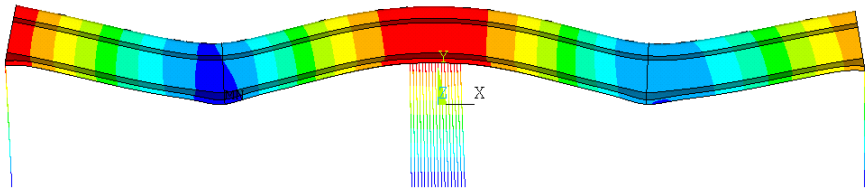

Fig. 15. The mode shapes corresponding to frequency ω_3 (the second FE model of the railway rail, $l_p=(1/4)l_0$)

Summary

In the study a free transverse vibration analysis of the simply supported Timoshenko beam on an arbitrary variable Winkler foundation is presented. The analysis is based on the use of the analytical method compared with numerical simulation. The elastic foundation is composed of two arbitrary variable, massless, regions of the Winkler type. At first the general solution of free vibration is derived by the separation of variable method. The natural frequencies of the system under consideration are determined. Then the models of the system formulated by using finite element technique are prepared and eigenvalue problem is solved. Achieved results of calculation are discussed and compared for these models. All needed finite element models are formulated by using ANSYS FE code. It is important to note that the data presented in the article is yielded the practical advice to design engineers.